marked overlap of binding results in untreated and treated patients with the clinical diagnosis of PD, MSA or PSP. However, in those studies the investigators did not distinguish untreated from treated patients with parkinsonism. On the basis of our data, we propose that therapy with dopamine agonists, by reducing [^{123}I]IBZM binding, may in part account for the reported overlap (*8*). In agreement with this hypothesis, a recent study that compared patients with the clinical diagnosis of probable MSA or PSP with normal age-matched volunteers showed little or no overlap of specific [^{123}I]IBZM binding (*4*).

CONCLUSION

Treatment with L-Dopa does not influence [^{123}I]IBZM binding, at least after a period of 3–6 mo, whereas dopamine agonists can reduce [^{123}I]IBZM binding. Because the reduction in specific ^{11}C-raclopride under treatment with a dopamine agonist reversed after a drug holiday of 3 days (*9*), we propose that these drugs be stopped about 7 days before an [^{123}I]IBZM SPECT investigation. Under this condition, [^{123}I]IBZM SPECT should equally predict dopaminergic responsiveness in patients previously treated with dopamimetic drugs compared with previously untreated patients. Reduction of specific [^{123}I]IBZM binding during treatment with a dopamine agonist most likely does not correlate with a functional striatal defect; rather, it reflects a pharmacological effect.

REFERENCES

1. Schwarz J, Tatsch K, Arnold G, et al. Iodine-123-iodobenzamide-SPECT predicts dopaminergic responsiveness in patients with "de novo" parkinsonism. *Neurology* 1992;42:556–561.
2. Quinn N. Multiple system atrophy: the nature of the beast. *J Neurol Neurosurg Psychiatry* 1989;52(suppl):78–89.
3. Schulz JB, Klockgether T, Petersen D, et al. Multiple system atrophy: natural history, MRI morphology and dopamine receptor imaging with [^{123}I]IBZM SPECT. *J Neurol Neurosurg Psychiatry* 1994;57:1047–1056.
4. van Royen E, Verhoeff NF, Speelman JD, Wolters EC, Kuiper MA, Janssen AG. Multiple system atrophy and progressive supranuclear palsy: diminished striatal dopamine-D2 receptor activity demonstrated by [^{123}I]IBZM single-photon emission computed tomography. *Arch Neurol* 1993;50:513–516.
5. Wenning GK, Ben Shlomo Y, Magalhaes M, Daniel SE, Quinn NP. Clinical features and natural history of multiple system atrophy: an analysis of 100 cases. *Brain* 1994;117:835–845.
6. Brücke T, Podreka I, Angelberger P, et al. Imaging of dopamine D2 receptors with SPECT: studies in patients with extrapyramidal disorders and under neuroleptic treatment. *J Cereb Blood Flow Metab* 1991;11:220–228.
7. Brooks DJ, Ibanez V, Sawle GV, et al. Striatal D2 receptor status in patients with Parkinson's disease, striatonigral degeneration and progressive supranuclear palsy, measured with ^{11}C-raclopride and positron emission tomography. *Ann Neurol* 1992; 31:184–192.
8. Schelosky L, Hierholzer J, Wissel J, Cordes M, Poewe W. Correlation of clinical response in apomorphine test with D2 receptor status as demonstrated by [^{123}I]IBZM SPECT. *Mov Disord* 1993;8:453–458.
9. Antonini A, Schwarz J, Oertel WH, Beer HF, Madeja UD, Leenders KL. Carbon-11-raclopride positron emission tomography in previously untreated patients with Parkinson's disease: influence of L-Dopa and lisuride therapy on striatal dopamine D2 receptors. *Neurology* 1994;44:1325–1329.
10. Gibb WRG, Lees AJ. The relevance of the Lewy body to the pathogenesis of idiopathic Parkinson's disease. *J Neurol Neurosurg Psychiatry* 1988;51:745–52.
11. Tatsch K, Schwarz J, Oertel WH, Kirsch CM. SPECT imaging of dopamine D2 receptors with [^{123}I]IBZM: initial experiences in controls and patients with Parkinson syndromes and Wilson's disease. *Nucl Med Commun* 1991;12:699–701.
12. Hughes AJ, Lees AJ, Stern GM. Challenge test to predict the dopaminergic response. *Neurology* 1991;41:1723–1725.
13. Gasser T, Schwarz J, Arnold G, Trenkwalder C, Oertel WH. Apomorphine test for dopaminergic responsiveness in patients with previously untreated Parkinson syndrome. *Arch Neurol* 1992;49:1131–1134.
14. Oertel WH, Gasser T, Trenkwalder C, Ippisch R, Poewe W. Apomorphine test for dopaminergic responsiveness. *Lancet* 1989;1:1262–1263.

Determination of Regional Rate Constants from Dynamic FDG-PET Studies in Parkinson's Disease

M. Piert, R.A. Koeppe, B. Giordani, S. Minoshima and D.E. Kuhl

Division of Nuclear Medicine, Department of Internal Medicine and Neuropsychology Program, University of Michigan Medical Center, Ann Arbor, Michigan

Dynamic [^{18}F]fluorodeoxyglucose (FDG) PET was used in Parkinson's disease patients and normal controls to determine kinetic rate constants for FDG. The goal was to assess whether the metabolic decreases observed in Parkinson's disease are associated with transport or phosphorylation processes or both. **Methods:** Fluorine-18-FDG was administered to 18 Parkinson's disease and 15 normal control subjects. Dynamic PET scanning was performed for 1 h and rate constants were obtained by nonlinear, least-squares analysis. Regional glucose metabolic rate was calculated from the individually fitted rate constants and by two standard static scan analyses. **Results:** Global CMRglu was decreased in Parkinson's disease (mean reduction 22%), reaching statistical significance in all regions investigated. K_1 was significantly reduced in parietal cortex, temporal cortex and striatum while k_3 was significantly reduced only in parietal cortex. The rate constant k_2 was unchanged. **Conclusion:** K_1, k_3 and CMRglu all demonstrated greater deficits across the brain with progression of disease and development of dementia, particularly in the parietal and occipital cortex. This suggested that the metabolic disturbance may be a global dysfunction throughout the brain. Because altered rate constants are specifically taken into account, dynamic measurements has shown to provide higher sensitivity for detecting diminished glucose utilization in Parkinson's disease than static approaches.

Key Words: Parkinson's disease; dementia; kinetic rate constants; glucose metabolism

J Nucl Med 1996; 37:1115–1122

In Parkinson's disease, little gross structural brain damage accompanies a specific biochemical lesion of the substantia nigra and its dopaminergic projections in the striatum (*1*). In living parkinsonian patients, PET has provided valuable pathophysiological information concerning altered pre- and postsynaptic compartments of the striatal dopaminergic neurotransmitter system (*2–4*). In early asymmetrical Parkinson's disease patients, [^{15}O]O_2 and [^{18}F]fluorodeoxyglucose (FDG) PET

Received Jun. 12, 1995; revision accepted Oct. 8, 1995.

For correspondence or reprints contact: Robert A. Koeppe, PhD, Division of Nuclear Medicine, 3480 Kresge III, Box 0552, University of Michigan, Ann Arbor, MI 48109.

studies found relatively increased cerebral oxygen and glucose metabolism in the lentiform nucleus contralateral to the more affected limb (*5,6*). FDG studies in bilateral Parkinson's disease showed a mild global glucose hypometabolism (*7–9*), without selective metabolic change in the striatum. In Parkinson's disease with dementia (PDD), there was a more marked global decline in glucose metabolism accompanied by a pattern of parietal hypometabolism similar to that seen in Alzheimer's disease (*7–10*). Eidelberg et al. (*11*) found a significant decrease of the mean K_1 in the nondemented parkinsonian brain (n = 13) on dynamic PET scans, whereas mean k_2 and k_3 values were not different from controls. More recently, Eidelberg et al. (*12*) were unable to show significant differences in gray-matter rate constant estimates and striatal CMRglu in Parkinson's disease (n = 7), whereas CMRglu was significantly reduced in caudate and putamen in patients with nigro-striatal degeneration, compared to Parkinson's disease and normal controls.

Structural and functional changes in degenerative brain disorders may influence glucose transport as well as certain subsequent steps in the metabolism of glucose. In spite of these potential effects, calculations of CMRglu from static FDG studies generally are based on both standard rate constants and a lumped constant obtained from healthy young volunteers (*13*). Whereas the lumped constant is considered to be less variable in severely affected brain (*14*), Lammertsma et al. (*15*) and others have pointed out that using standard rate constants in static imaging is acceptable only when the magnitude of metabolic change is sufficient to be detected and when the rate constants differ only slightly from those of controls. Dynamic PET allows the evaluation of the basic mechanisms of regional glucose metabolism by estimating forward and reverse glucose transport (K_1 and k_2) as well as the initial intracellular metabolic step, the phosphorylation of FDG by hexokinase (k_3). The hydrolysis of FDG-6-phosphate back to free FDG described by k_4, can be estimated, but is imprecisely determined from dynamic sequences of only 1 hr.

We have used dynamic PET to evaluate whether the regional glucose hypometabolism present in Parkinson's disease is associated with a glucose transport deficiency and/or with an alteration of metabolism at the hexokinase step. Furthermore, we investigated whether the suspected alteration of the metabolic rate constants affects the accuracy of the static measurement of the CMRglu by comparing results from a kinetic analysis with those from two common static approaches (*13,16*) and two different sets of standard rate constants.

MATERIALS AND METHODS

Subjects

PET data were collected from 18 patients with Parkinson's disease (age 43–78 yr; mean ± s.d. = 66 ± 9; duration of disease 1–19 yr; mean ± s.d. = 9 ± 5) and 15 normal control subjects (age 51–79 yr; mean ± s.d. = 65 ± 10). Overall disease severity was rated by the Hoehn and Yahr scores (H&Y scores) (*17*) and ranged from 1 to 5 (mean ± s.d. = 3.2 ± 1.1). Each patient's cognitive impairment was graded by the Mini-Mental State Examination (*18*) (MMSE; range 30–5, mean ± s.d. = 23 ± 7) and Clinical Dementia Rating (*19*) (CDR; range 0–2, mean ± s.d. = 0.6 ± 0.7). Eleven of eighteen Parkinson's disease subjects (61%) were considered to be either questionably demented (CDR 0.5) or mildly to moderately demented (CDR 1,2).

General medical and neurological examinations were performed along with several laboratory tests to exclude thyroid disease, and vitamin B12 or folate deficiency were performed. Further exclusionary criteria for both patients and elderly control subjects included: cerebrovascular disease, diabetes mellitus or hyperglycemia (plasma glucose level >125 mg/100 ml plasma during the scan), previous cranial trauma, encephalitis, drug or alcohol abuse, mental retardation, family history of neurologic or psychiatric illness or dementing disease. With the exception of one Parkinson's disease subject, all patients received levodopa alone or in combination with bromocriptine. Patients were included in the study only if the initial presentation was at least 1 yr prior to the scan. Patients taking anti-parkinsonian drugs remained on these medications during the PET study. Patient history and test data are summarized in Table 1. The patients age at study and gender distribution were not significantly different between patient and control groups. Parkinson's disease patients with greater overall disease severity (as measured by H&R scores) tended to have a greater cognitive impairment (MMSE) as well as a higher rating of dementia than patients assessed to have less severe disease.

The present study includes data from either of two PET tomographs (tomograph 1: Siemens ECAT 931/08-12; tomograph 2: Cyclotron Corp. PC 4600 Neuro-PET). PET data of 10 Parkinson's disease patients (mean age ± s.d. = 66 ± 7) and 10 normal control subjects (age = 67 ± 14) were obtained with tomograph 1. The remaining subjects, eight Parkinson's disease (age = 67 ± 8) and five normal control subjects (age = 62 ± 4), were scanned on tomograph 2.

Ethical permission for this study was obtained from the Institutional Review Board of the University of Michigan. All subjects or legal guardians gave their written consent after thorough explanation of the entire experimental procedure.

Radiotracer

Fluorine-18-FDG was routinely prepared by direct nucleophilic exchange on a quaternary 4-aminopyridium resin (*20*). Radiochemical purity, as assessed by a thin-layer chromatography, was uniformly greater than 97%. Radioactivity at time of injection was 10 ± 1 mCi in each subject.

Scanning Procedure

Scans were performed either on tomograph 1 with a reconstructed in-plane resolution of approximately 7 mm FWHM and 7–8 mm FWHM in axial direction, or on tomograph 2 with reconstructed in-plane resolution of approximately 12 mm FWHM and 10 mm FWHM axially (*21*). Each subject was examined in a fasting state with eyes open, ears unplugged in a quiet and moderately lighted room. Subjects were placed in a comfortable supine position, restrained by a small band across the forehead. No patients required sedation for the examination. A 10 ± 1-mCi dose of FDG was administered uniformly over a period of 30 sec. A dynamic sequence of 15 PET scans over 60 min was performed for each subject according to the following protocol: 4 × 0.5 min, 3 × 1 min, 2 × 2.5 min, 2 × 5 min, 4 × 10 min. The scanned field-of-view included 10 cm for tomograph 1 and 5.5 cm for tomograph 2, starting at 1.0 cm and 2.0 cm above the canthomeatal line, respectively. Arterial blood samples from the forearm, opposite to the site of injection, were drawn into heparinized syringes as rapidly as possible for the first 2 min following the injection and then at progressively longer intervals throughout the remainder of the study. Plasma was separated and radioactivity was counted in a NaI(T1) well-counter. Three plasma samples were averaged to determine the glucose level during the time of the scan using standard enzymatic methods. Subjects with unstable glucose levels during the scan (difference > 20 mg/100 ml plasma between any two samples) were excluded from the study.

Image Processing

The images corrected for attenuation by a standard calculated method using a series of ellipses. Final images were reconstructed

TABLE 1
Patient Data

Patient no.	Age (yr)	Sex	Duration	Medication	H&Y	CDR	MMSE
1	64	Male	8	L	1	0	30
2	64	Male	9	L	2	0	30
3	63	Male	7	L	2	1	21
4	67	Male	4	L	2	1	20
5	43	Male	18	L,B	3	0	30
6	59	Female	6	L	3	0	28
7	71	Male	5	L	3	0	28
8	66	Male	8	L	3	0	28
9	62	Female	8	L	3	0	26
10	58	Male	1	L,B	3	0.5	29
11	76	Female	6	L	3	0.5	23
12	79	Female	12	L	3	1	21
13	57	Male	4	NONE	3	1	24
14	64	Male	19	L,B	4	0.5	27
15	76	Male	14	L	4	1	20
16	65	Male	9	L	5	1	17
17	78	Male	12	L	5	2	10
18	72	Female	14	L	5	2	5

H&Y = Hoehn & Yahr Score; CDR = clinical dementia rating; MMSE = mini-mental state examination; L = levodopa; B = bromocriptine.

onto a 128 × 128 pixel grid for the entire dynamic sequence (total: 15 frames × 15 planes or 5 planes). Radioactive fiducial markers were placed on the patient's scalp and an automated motion correction routine was used to define the marker locations on a single frame and then reorient all other frames to the base frame (*22*). Radioactivity concentrations measured in tissue and plasma were corrected for decay and adjusted for the time shift between brain and radial artery.

Cerebral cortical regions of interest (ROIs) were individually drawn according to a standard neuroanatomical (*23*). A computerized tomography atlas for the right and left striatum, right and left frontal cortex, right and left temporal cortex, right and left parietal cortex, and a single occipital region predominantly located in Brodmann's areas 18 and 19, excluding most of primary visual cortex (Brodmann area 17) were also individually drawn. All cortex regions are located along the cortical surface and extend no more the 15 mm inwards from the surface. Since only small differences were found between the hemispheres and no tendency for left/right asymmetry was observed in either right- or left-handed subjects, homologous ROIs were averaged to yield mean regional rate constants and metabolic rates for all regions.

Mathematical Model

In both groups, kinetic parameters were estimated from the tissue (dynamic PET) and arterial plasma (discrete samples) radioactivity curves by a standard nonlinear least-squares analysis using the Marquardt algorithm (*24,25*). A standard three-compartment tracer kinetic model (*13,16*) extending the original method of Sokoloff et al. (*26*) was used. Parameters K_1 (blood brain^{-1} min^{-1}) and k_2 (min^{-1}) describe forward and backward tracer transport across the blood-brain barrier. Parameters k_3 (min^{-1}) and k_4 (min^{-1}) describe phosphorylation and dephosphorylation of FDG within the tissue compartments. In addition to the four rate constants K_1-k_4, the fractional cerebral blood volume CBV, was estimated in the least-squares fit in order to correct for blood-borne activity in the PET measurement. Kinetic CMRglu, given in units of mg glucose 100 ml brain^{-1} min^{-1}, was calculated directly from the individual's fitted rate constants and averaged plasma glucose concentration (Cp; mg glucose 100 ml blood^{-1}) measure and a fixed lumped constant value of 0.52 (*27*) as follows:

$$\text{CMRglu} = \frac{\text{Cp}}{\text{LC}} \times \frac{k_1 \times k_3}{k_2 + k_3}.$$

To compare different static CMRglu measurement approaches with CMRglu obtained from the individually fitted rate constants, we estimated static CMRglu from a summed image containing data from 30 to 60 min postinjection in the 10 Parkinson's disease and 10 normal control subjects scanned on tomograph 1. Static CMRglu was then calculated with a lumped constant of 0.52 applying two different methods: U = UCLA method (*13*), W = Wisconsin method (*16*); and two sets of standard rate constants (set 1: K_1 = 0.084, k_2 = 0.193, k_3 = 0.096, k_4 = 0.007 from normals controls scanned previously at the University of Michigan, and set 2: K_1 = 0.102, k_2 = 0.130, k_3 = 0.062, k_4 = 0.0068 (*13*) resulting in four different static approaches (W1 = Wisconsin method and rate constant set 1; W2 = Wisconsin method and rate constant set 2; U1 = UCLA method and rate constant set 1; U2 = UCLA method and rate constant set 2).

Both static methods use a formula that is based on a set of standard or population average rate constants (given above) plus a factor to correct for the difference between the FDG concentration predicted by the population average rate constants and that actually measured by PET. The UCLA method uses a correction factor given by the ratio of the individual's regional tracer concentration in the *phosphorylated* compartment to that predicted by calculations from the population average rate constants, while the Wisconsin method uses a factor given by the ratio of the individual's measured *total* tracer concentration to that predicted by from calculations using the population average rate constants. Which method will perform with higher accuracy depends upon which rate constants in patient subjects will vary more from the control population average values. In general, the UCLA method provides a more accurate estimate of metabolic rate when there are differences in the phosphorylation-related parameter k_3, while the Wisconsin method yields better results when there are changes in transport-related parameters K_1 and/or k_2 (*16*).

Statistical Analysis

The values reported represent the arithmetic mean of both hemispheres and the s.d. across subjects. Since estimates of individual rate constants are quite high for dynamic FDG studies,

we analyzed as many subjects as possible to increase statistical power, and thus have included results from subjects scanned on two different scanners. To compare data obtained from tomographs with different resolution and counting efficiency, we normalized the individual results of the fitted rate constants and the kinetic CMRglu to the mean value of the normal control group obtained on each tomograph. Following this step, the mean value in each region for the control group becomes 1.0, yet the correct s.d. and coefficients of variation are maintained since each individual (both control and patient) was adjusted by the normal group mean. This approach is appropriate mathematically since data from the two scanners have exhibited nearly identical inter-subject variability in both the control and patient groups (*28–30*), yet the global means of the CMRglu and individual rate constants measured with the new tomograph were ~10% higher than the old scanner. Normalized rate constants and metabolic rates in all brain regions were compared by means of analysis of variance, including the Bartlett test for homogeneity of group variances. In the case of equal variances, selecting a conservative significance level ($p \geq 0.1$), data were compared by the Tukey studentized range method. In case of unequal variances ($p < 0.1$) Student's t-tests for differences between groups with unequal variances were performed based on the Behrens-Fisher t′ distribution.

We performed stepwise regression analysis to describe the accuracy of different static approaches in their ability to yield the same results as those obtained from the dynamic CMRglu calculation, and to determine the correlation coefficient between kinetic and static methods. All statistical tests were corrected for multiple comparisons. Differences between groups were considered significant when comparisons exceeded 95% confidence limits ($p < 0.05$). Statistical tests were performed with either the BMDP, SAS or Statview statistical software packages.

RESULTS

Figure 1 plots regional means and standard deviations for the estimates of dynamic FDG rate parameters and metabolic rate in Parkinson's disease versus normal control in the seven brain regions. Values are for each group are expressed as a percent of the normal control group mean, as described previously, to allow combining data from the two different scanners. The uncertainties in the parameter estimates varied between groups, across the various ROIs, and across the different kinetic parameters, as can be seen by the s.d. plotted in Figure 1. Variability (expressed as the coefficient of variance; COV = s.d./mean) was lowest in K_1 and CMRglu in all regions for both groups with COVs ranging 14% (for K_1 in temporal cortex of both normal controls and Parkinson's disease to 30% (for K_1 in thalamus of Parkinson's disease). Uncertainties in k_2 and k_3 estimates are substantially higher, ranging from 24% (for k_3 in cerebellum of Parkinson's disease) to 58% (for k_2 in thalamus of Parkinson's disease). Rate constant and CMRglu uncertainties were distributed across nearly equivalent ranges for both PET scanners.

Results showed a quite uniform decrease in K_1, k_3 and CMRglu, but not k_2, for Parkinson's disease compared to normal controls. In Parkinson's disease, CMRglu was found to be reduced in all cortical and subcortical brain regions compared to normal control subjects with a mean reduction: 22%. Kinetic CMRglu reductions reached statistical significance in the striatum (25%); thalamus (22%), as well as the frontal (20%), parietal (29%), temporal (23%), and occipital cortices (19%) and cerebellar cortex (18%). Estimates of the rate constant K_1 were significantly decreased in the parietal (17%), temporal cortex (15%) and striatum (15%). Decreases were observed in all other regions ranging from 6% in the cerebellum

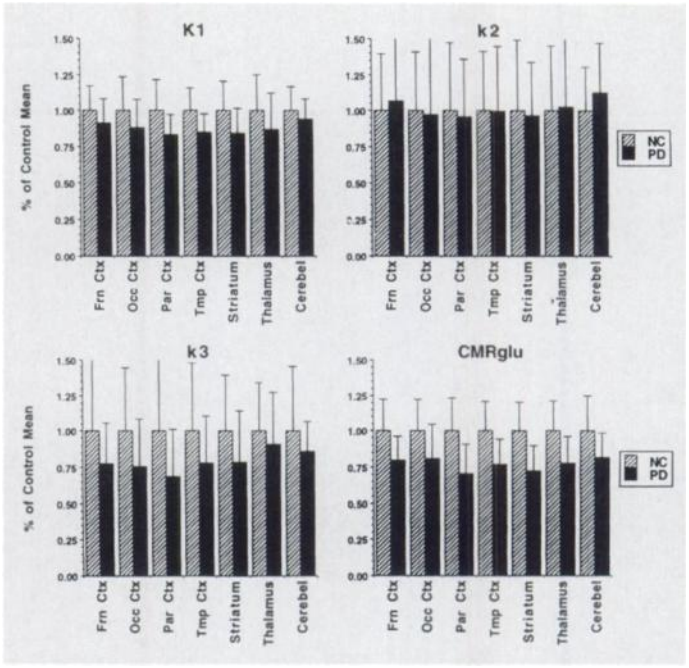

FIGURE 1. Regional estimates of dynamic FDG rate parameters and metabolic rate in Parkinson's disease (n = 18) and elderly normal control subjects (n = 15). Values are mean and s.d. for each group expressed as a percent of the normal control group mean.

to 13% in the occipital cortex, but were not significant after adjustment for multiple comparisons. No significant changes or trends toward decreases were observed in any region for k_2. Mean estimates of the rate constant k_3 were reduced in all regions, however due to the high intersubject variability, statistical significance adjusted for multiple comparisons was achieved only in the parietal cortex (32%). Reductions in k_3 ranging from 21% to 25% ($p < 0.05$ prior to multiple comparison adjustment) were observed in striatum and frontal, temporal, and occipital cortices. Smaller decreases were observed in cerebellum (14%) and thalamus (9%).

We separately examined the subgroup of Parkinson's disease patients without dementia (CDR = 0; n = 7). In this group, the mean decrease in CMRglu relative to normal controls averaged 17% (compared to a 22% decrease for the entire group). Mean regional decreases ranged from 10%–22% compared to 15%–29% for the entire group. With correction for multiple comparisons, significant CMRglu differences in this subgroup were detected only in striatum and parietal cortex. The loss of significance in the other regions, however, was caused as much by the smaller sample size (n = 7 versus n = 18 for the entire group) as by the actual magnitude of the decrease (i.e., 18% in the nondemented group compared to 20% in the entire group in frontal cortex or 15% compared to 18.0% in cerebellum). Slightly smaller decreases in K_1 relative to normals were also observed in the nondemented subgroup than were observed in the entire group. Only the decrease in putamen remained significant (17%). Decreases were no longer significant in parietal and temporal cortex. As was observed for the entire group, no significant differences in k_2 were detected for the nondemented Parkinson's disease subgroup compared to normals. The rate constant k_3 was still reduced in all regions in the nondemented subgroup, however the deficit in parietal cortex was no longer significant, averaging only a 23% reduction compared to 32% for the whole group. Reductions in k_3 in temporal and occipital cortex were also smaller in the nondemented subgroup (19% compared to 25% for the entire group in temporal and 14% compared to 22% in occipital cortex).

Similar magnitude decreases were observed in the subgroup for striatum (19 versus 21%), frontal cortex (25 versus 23%), cerebellum (15 versus 14%) and thalamus (8 versus 9%).

We performed regression and correlational analyses using the patient data given in Table 1 and each of the regional rate parameters from PET (K_1, k_2, k_3, CMRglu). No significant correlations were found between either patient age or duration of illness and any of the four PET parameters in any region examined. The three clinical measures of disease severity were significantly interrelated, with CDR and MMSE correlating at 0.94, and H&Y scores correlating with CDR and MMSE at 0.62 and 0.64, respectively. Since the major PET findings demonstrated global decreases in the K_1, k_3 and CMRglu with only secondary regional variations, the PET measures declined with worsening CDR, MMSE or HYS, in the majority of regions examined. CDR correlated significantly with decreased K_1 in parietal ($p < 0.05$) and occipital ($p < 0.01$) cortex, decreased k_3 in striatum ($p < 0.05$), and decreased CMRglu in parietal, occipital and temporal cortex ($p < 0.05$). Due to the very high correlation between CDR and MMSE, regression of the PET data with MMSE yielded similar results. MMSE correlated significantly with K_1 in parietal ($p < 0.05$) and occipital ($p < 0.01$) cortex, with k_2 and k_3 in occipital cortex ($p < 0.05$), and with CMRglu in parietal ($p < 0.01$), occipital ($p < 0.01$) and temporal cortex ($p < 0.05$). Figure 2 shows regression of MMSE with occipital cortex for each of the four PET parameters. The H&Y scores score correlated more poorly with PET, reaching significance only for striatal CMRglu.

Kinetic measurement is considered to provide a less biased estimate of the true CMRglu than static imaging because individual rate constants are taken into account (*15,31*). To investigate the effect of altered glucose rate constants on the accuracy of static FDG-PET, we compared the kinetic CMRglu with different static methods from data obtained on the ECAT 931 tomograph, using stepwise regression analysis (Table 2). In general, kinetic CMRglu was highly correlated with all four of the static measures in both patients and normal control subjects (correlation coefficient $r > 0.85$). Due to a few individual cases in the patient groups where rate constants were distinctly abnormal, the correlation dropped in the frontal cortex ($r > 0.78$) and thalamus ($r > 0.72$). Taking the kinetic values as a gold standard, static measures overestimated CMRglu in all cases, in normal control subjects ranked as follows: kinetic CMRglu < W2 < W1 < U2 < U1 (static approaches).

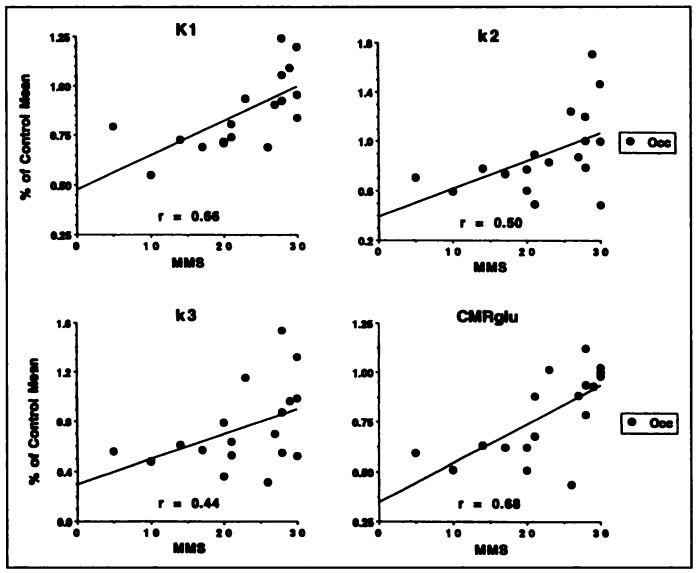

FIGURE 2. Regression of the mini-mental state examination score (MMSE) with the estimated FDG rate parameters in occipital cortex for the 18 Parkinson's disease patients. Correlations with regional K_1 and CMRglu are higher than those with k_2 or k_3 due to the higher parameter estimation uncertainty associated with these latter two parameters.

In the Parkinson's disease group, the rank order of the estimates from the U2 and W1 approaches were switched in most regions, with the U2 method yielding values closer to the kinetic estimates of CMRglu. The UCLA method enhances differences in K_1 and k_2 (*16*) causing the decreases in K_1 seen in Parkinson's disease to be enhanced, in part cancelling the overestimations seen in normal controls and making them more consistent with the kinetic values. Comparing the regional CMRglu in Parkinson's disease to that in normal control subjects, we no longer detected significant reductions of the CMRglu in the static approaches in one region, cerebellar cortex, using standard rate constants for the calculations. The levels of significance for the other six regions which remained statistically significant using the static approaches were always lower than when using the kinetic approach. Using stepwise regression analysis, however, none of the four combinations of static method and rate constant set was found to predict the kinetic CMRglu more accurately than any other combination.

DISCUSSION

Parkinson's disease is pathologically characterized by the degeneration of the substantia nigra and its dopaminergic projections to the striatum (*32*). Glucose metabolism in Parkinson's disease has been found to be reduced globally in bilaterally affected Parkinson's disease in the current study as well as by other investigators (*7,9,12*). Since Parkinson's disease is known to involve the striatum, a decline in striatal CMRglu was expected to be observed in Parkinson's disease and PDD. FDG studies, however, have consistently failed to show specific focal striatal reductions of CMRglu, whereas uptake of [^{18}F]fluorodopa in Parkinson's disease patients has been found to be significantly reduced in putamen and caudate nucleus (*4,33*). This inconsistency has been explored, and it may be that the reduction of dopaminergic synaptic activity, accounting for only about 20% of all striatal synapses, may be too small to affect significantly the measured rate of glucose metabolism in caudate and putamen (*7*).

Using dynamic PET measures, we identified a moderate global reduction of the glucose utilization in cortical and subcortical structures in a group of 18 Parkinson's disease patients compared to 15 age-matched controls (mean reduction = 22%). Uniform reductions occurred in all regions and was slightly greater in the parietal cortex and striatum than in other regions. These global findings are consistent with previous works (*7,17*) who reported global reduction in CMRglu in about 20%. The enhanced parietal decrease, observed in our data, was caused by a few of the more severe patients with greater cognitive impairment having metabolic patterns indicative of Alzheimer's disease. The subset of Parkinson's disease subjects with CDR = 0 exhibited smaller decreases in CMRglu (mean reduction = 17%) than did the entire group. Smaller decreases were also observed in the transport and phosphorylation rate parameters for this subgroup, particularly in parietal, temporal, and occipital cortices, while the observed decreases in the striatum, thalamus, striatum and frontal cortex were of nearly equal magnitude for both nondemented and demented subgroups.

In the nigro-striatum, the more pronounced hypometabolism could reflect the well defined structural changes the occur with degeneration of neurons, reduced dendritic branching, axon degeneration and consequently loss of synaptic activity. Al-

TABLE 2

CMRglu (mg · 100 $ml^{-1}min^{-1}$) Estimates in Parkinson's Disease Patients Compared to Normal Controls*

Region	Group				Parkinson's disease/ Normal controls
	Controls (n = 10)		Parkinson's disease (n = 10)		
	Mean	s.d.	Mean	s.d.	
Cerebellar cortex					
Kinetic CMRglu	7.98	1.71	6.24	1.27†	0.78
Static CMRglu U1	9.20	1.77	7.91	1.21	0.86
Static CMRglu U2	8.90	1.91	7.27	1.17	0.82
Static CMRglu W1	8.54	1.59	7.52	0.98	0.88
Static CMRglu W2	7.99	1.50	6.98	0.90	0.87
Frontal cortex					
Kinetic CMRglu	8.10	1.90	6.08	1.23‡	0.75
Static CMRglu U1	9.64	2.35	7.56	1.41†	0.78
Static CMRglu U2	9.17	2.33	6.95	1.37†	0.76
Static CMRglu W1	8.78	2.00	7.09	1.28†	0.81
Static CMRglu W2	8.20	1.87	6.61	1.21†	0.81
Occipital cortex					
Kinetic CMRglu	7.10	1.53	5.71	1.56‡	0.80
Static CMRglu U1	8.35	1.76	6.88	1.36†	0.82
Static CMRglu U2	7.85	1.80	6.25	1.29†	0.80
Static CMRglu W1	7.69	1.50	6.48	1.24†	0.84
Static CMRglu W2	7.19	1.40	6.06	1.15†	0.84
Parietal cortex					
Kinetic CMRglu	7.52	1.42	5.32	1.23‡	0.71
Static CMRglu U1	8.77	1.92	6.48	1.15‡	0.74
Static CMRglu U2	8.28	1.96	5.87	1.27‡	0.71
Static CMRglu W1	8.05	1.64	6.19	1.09‡	0.77
Static CMRglu W2	7.52	1.54	5.77	1.01‡	0.77
Striatum					
Kinetic CMRglu	9.48	1.85	6.53	1.43‡	0.69
Static CMRglu U1	11.78	2.91	8.62	1.37‡	0.73
Static CMRglu U2	11.36	2.98	8.03	1.32‡	0.71
Static CMRglu W1	10.56	2.47	7.94	1.14‡	0.75
Static CMRglu W2	9.86	2.31	7.43	1.09‡	0.75
Temporal cortex					
Kinetic CMRglu	7.99	1.77	6.38	1.52‡	0.80
Static CMRglu U1	9.35	2.04	7.66	1.41†	0.82
Static CMRglu U2	8.87	2.07	7.05	1.40†	0.80
Static CMRglu W1	8.52	1.73	7.11	1.24†	0.83
Static CMRglu W2	7.97	1.64	6.69	1.16†	0.84
Thalamus					
Kinetic CMRglu	9.27	2.78	6.99	1.42†	0.75
Static CMRglu U1	11.48	3.52	9.18	1.75	0.80
Static CMRglu U2	11.14	3.42	8.61	1.64†	0.77
Static CMRglu W1	10.40	2.81	8.44	1.36†	0.81
Static CMRglu W2	9.75	2.66	7.87	1.37†	0.81

*Also given are CMRglu estimates from four static approaches.

†$p < 0.05$, ‡$p < 0.01$.

though Lewi bodies have been found in cortical structures (*1,35*), prominent pathologic changes in cortex have not been described in Parkinson's disease. Alternatively, cortical hypometabolism may be related to functional abnormalities in the absence of major structural change. Peppard (*9*) proposed a cascade effect of reduced activity mediated through cortical interneurons and cortico-cortical connections. Quantitative morphologic studies in Parkinson's disease indicate that in addition to the nigro-striatal cell damage, noradrenergic, serotonergic and cholinergic systems are involved, causing multiple neuromediator dysfunctions (*1*). In more advanced parkinsonism with dementia, cell loss and the reduction of noradrenalin, serotonin and cholinergic markers are more severe than in early Parkinson's disease (*36,37*). Our data suggests a widespread effect of the nigro-striatal degeneration on the glucose metabolism throughout the entire parkinsonian brain.

The reduction of the CMRglu in Parkinson's disease was accompanied by a decline of both K_1 and k_3 in all regions investigated, most significantly in parietal cortex, temporal cortex, and striatum. The observed high inter-individual variabilities of rate constant estimates are consistent with those reported for young (*13,38*) and elderly normal volunteers (*14,39,40*). Eidelberg et al. (*11*) found a significant global decline of K_1 in a group of 13 Parkinson's disease patients,

while mean global rate constant estimates for k_2 and k_3 were not significantly altered. Regional rate constant estimates, however, were not reported. In a more recent study, Eidelberg et al. (*12*) were unable to detect any differences in rate constants ($K_1 - k_3$) in 7 Parkinson's disease patients compared to 15 normal control subjects. Our data suggest that their lack of significant results may be attributable to the high inter-individual variability of rate constant estimates in conjunction with the limited number of subjects studied. Regional variability of the rate constant estimates decreases the probability of detecting differences between groups when averaging gray matter estimates across brain regions as was done by Eidelberg et al. (*12*). Another contributing factor is that 50% of our patient group have at least mild dementia.

A marked parietal glucose hypometabolism, as was observed in Alzheimer's disease, has been identified as the primary difference between Parkinson's disease and PDD in previous static FDG studies (*7–10*). Only the cerebellar cortex was relatively spared in PDD. These data are in good agreement with a recent static FDG study, reporting widespread metabolic reduction in PDD including the occipital region, but excluding the cerebellar cortex (*41*), which might suggest a different metabolic pattern compared to Alzheimer's disease, where the occipital cortex is less affected. Our data suggest that the enhanced hypometabolism in PDD, predominantly in cortical regions, is caused by a further reduction of both glucose transport (K_1) and phosphorylation at the hexokinase step (k_3) relative to Parkinson's disease, but due to the smaller number of patients with more prominent cognitive deficits, statistically significant results in this subgroup of patients could be achieved only in the most affected region of the brain, parietal cortex.

The underlying mechanisms for the reduction of glucose influx and phosphorylation in Parkinson's disease are poorly understood. Hexose transporters, which have been found reduced in brain biopsies of Alzheimer's disease patients (*42*), have not, as of yet, been determined in Parkinson's disease or PDD subjects. Therefore, we can only speculate that the reduction of K_1 might be related to a reduced number of glucose transporters in affected areas of Parkinson's disease. Equation 1, however, allows other possible explanations for the reduction of glucose influx. Since K_1 is the product of regional CBF and the single-pass capillary extraction fraction, reduced cerebral blood flow will cause a decrease in K_1, but possibly of lesser magnitude since the extraction fraction might undergo a concomitant increase. In Parkinson's disease, the reported flow reduction of approximately 20% (*6*) is consistent with our observed K_1 reductions of approximately 15%. These reductions in K_1 are too small to explain the observed decline of CMRglu. By using Equation 1 and population average rate constants, a simple fixed reduction in flow (i.e., causing comparable reductions in both K_1 and k_2) is shown to cause a 2.5 times smaller reduction in the CMRglu, when k_3 remains unchanged. Therefore, a decrease in k_3 also is necessary to explain the reductions in CMRglu of approximately 20%–30% in the striatum and cortex of Parkinson's disease subjects. Supporting this concept, we detected reductions in k_3 of up to 25% in the striatum and 29% in the parietal cortex.

In contrast to Alzheimer's disease, where a reduced hexokinase activity has been measured in affected areas (*43*), hexokinase activity deficiencies have not been demonstrated previously in Parkinson's disease. Nevertheless, our results indicate that a combination of diminished glucose influx and phosphorylation at the hexokinase step contribute to the metabolic decline in Parkinson's disease in the most affected regions, and likely to some extent in all brain regions. It remains unclear whether the observed declines in glucose transport and phosphorylation are primarily deficiencies for the altered glucose metabolism or more likely the expression of functional down-regulation in a neuronal network, where energy demands are globally as well as regionally reduced.

To evaluate the effect of diminished glucose rate constants on the accuracy of static FDG-PET measurements, we compared the kinetic CMRglu with several static methods in data obtained on the higher resolution ECAT 931 tomograph. Although correlation between the kinetic and the different static approaches were generally comparably high, we no longer detected significant reductions of the CMRglu in one of seven regions examined in Parkinson's disease with any of the static approaches when using standard rate constants for the calculations. Furthermore, the level of significance was repeatedly lower for all static methods compared to kinetic measurements (Table 2). These data suggest, that kinetic measurement has a higher sensitivity in discriminating altered glucose metabolism, at least in small sample sizes, which are commonly observed in PET studies. Computer simulations studies of Huang et al. (*44*) pointed out that large differences in the rate constants K_1 to k_3 have dramatic effects on the CMRglu calculated by the operational equation of the Sokoloff FDG model. Our data suggest that the changes in K_1 and k_3 in Parkinson's disease are substantial enough to have caused a diminished sensitivity for detecting differences in metabolic rate between the Parkinson's disease patient group and normal controls. This result also suggests that the discrepancies between several previous static FDG studies and our kinetic CMRglu results may be explained by the use of standard rate constants and static methods.

CONCLUSION

We found a substantial global decrease in the metabolic rate in patients with Parkinson's disease. In the striatum and cortex of the parkinsonian brain, the declines in glucose utilization are accompanied by decreases in both glucose transport and hexokinase activity. Our results suggest that this metabolic disturbance may be a global dysfunction throughout the brain. With the progression of disease and the development of dementia with Parkinson's disease, metabolic declines are further pronounced, especially in the parietal cortex. Because altered rate constants are specifically taken into account, dynamic measurement have been shown to provide higher sensitivity for detecting diminished glucose utilization in Parkinson's disease, than static approaches.

ACKNOWLEDGMENTS

We thank Kathleen B. Welch and John Warner of the Center for Statistical Consultation and Research of the University of Michigan for their assistance. This study was supported in part by National Institutes of Health grants R01-NS-24896 and P01-NS-15655 awarded by NINDS and by Department of Energy grant DE-F602-87ER60561.

REFERENCES

1. Jellinger K. New developments in the pathology of Parkinson's disease. *Adv Neurol* 1990;53:1–16.
2. Garnett ES, Firnau G, Nahmias C. Dopamine visualized in the basal ganglia of living man. *Nature* 1984;305:137–138.
3. Wagner HN, Burns KD, Dannals RF, et al. Imaging dopamine receptors in the human brain by positron tomography. *Science* 1983;221:1264–1266.
4. Leenders KL, Palmer AJ, Quinn N, et al. Brain dopamine metabolism in patients with Parkinson's disease measured with positron emission tomography. *J Neurol Neurosurg Psychiatry* 1986;49:853–860.
5. Miletich RS, Chan T, Gillespie M, et al. Contralateral basal ganglia metabolism is abnormal in hemiparkinson patients. An FDG-PET study. *Neurology* 1988;38(suppl 1):S260.
6. Wolfson LI, Leenders KL, Brown LL, Jones T. Alterations of regional cerebral blood flow and oxygen metabolism in Parkinson's disease. *Neurology* 1985;35:1399–1405.

7. Kuhl DE, Metter EJ, Riege WH. Patterns of local cerebral glucose utilization determined in Parkinson's disease by the [^{18}F]fluorodeoxyglucose method. *Ann Neurol* 1984;15:419–424.
8. Kuhl DE, Metter EJ, Riege WH, Markham CH. Patterns of local cerebral glucose utilization in Parkinson's disease and Huntington's disease. *Ann Neurol* 1984; 15(suppl):S119–S125.
9. Peppard RF, Martin WR, Carr GD, et al. Cerebral glucose metabolism in Parkinson's disease with and without dementia. *Arch Neurol* 1992;49:1262–1268.
10. Kuhl DE, Metter EJ, Benson DF, et al. Similarities of cerebral glucose metabolism in Alzheimer's and Parkinsonian dementia. *J Cereb Blood Flow Metab* 1985;5(suppl 1):S169–S170.
11. Eidelberg D, Moeller JR, Dhawan V, et al. The metabolic anatomy of Parkinson's disease: complementary [^{18}F]fluorodeoxyglucose and [^{18}F]fluorodopa positron emission tomography studies. *Mov Disord* 1990;5:203–213.
12. Eidelberg D, Takikawa S, Moeller JR, et al. Striatal hypometabolism distinguishes striatonigral degeneration from Parkinson's disease. *Ann Neurol* 1993;33:518–527.
13. Phelps ME, Huang SC, Hoffman EJ, et al. Tomographic measurements of local cerebral glucose metabolic rate in humans with [^{18}F]2-fluoro-2-deoxy-D-glucose: validation of the method. *Ann Neurol* 1979;6:371–388.
14. Hawkins RA, Phelps ME, Huang S-C, Kuhl DE. Effect of ischemia on quantification of local cerebral glucose metabolic rate in man. *J Cereb Blood Flow Metab* 1981;1:37–51.
15. Lammertsma AA, Brooks DJ, Frackowiak RS, et al. Measurement of glucose utilization with [^{18}F]2-fluoro-2-deoxy-D-glucose: a comparison of different analytical methods. *J Cereb Blood Flow Metab* 1987;7:161–172.
16. Hutchins GD, Holden JE, Koeppe RA, et al. Alternative approach to single-scan estimation of cerebral glucose metabolic rate using glucose analogs, with particular application to ischemia. *J Cereb Blood Flow Metab* 1984;4:35–40.
17. Hoehn MM, Yahr MD. Parkinsonism: onset, progression and mortality. *Neurology* 1966;17:427–442.
18. Folstein MF, Folstein SE, Mc Hugh PR. Mini-Mental State: a practical method for grading the cognitive state of patients for the clinician. *J Psychiatr Res* 1975;12:189–198.
19. Berg L. Clinical dementia rating. *Psychopharmacol Bull* 1988;24:637–639.
20. Toorongian SA, Mulholland GK, Jewett DM, et al. Routine production of 2-deoxy-2-[^{18}F]fluoro-D-glucose by direct nucleophilic exchange on a quaternary 4-aminopyridinium resin. *Int J Rad Appl Instrum B* 1990;17:273–279.
21. Kearfott KJ, Carroll LR. Evaluation of the performance characteristics of the PC 4600 positron emission tomograph. *J Comp Assist Tomogr* 1984;8:502–513.
22. Koeppe RA, Holthoff VA, Frey KA, et al. Compartmental analysis of [^{11}C]flumazenil kinetics for the estimation of ligand transport rate and receptor distribution using positron emission tomography. *J Cereb Blood Flow Metab* 1991;11:735–744.
23. Talairach J, Tournoux P. Co-planar stereotaxic atlas of the human brain. Thieme, New York 1988.
24. Bevington PR. Data reduction and error analysis for the physical sciences. New York: Mc Graw-Hill; 1969:232–241.
25. Marquardt DW. An algorithm for least-squares estimation of nonlinear parameters. *J Soc Appl Math* 1963;11:431–441.
26. Sokoloff L, Reivich M, Kennedy C, et al. The [^{14}C]deoxyglucose method for the measurement of local cerebral glucose utilization: theory, procedure and normal values in the conscious and anesthetized albino rat. *J Neurochem* 1977;28:897–916.
27. Reivich M, Alavi A, Wolf A, et al. Glucose metabolic rate kinetic model parameter determination in humans: the lumped constants and rate constants for [^{18}F]fluorodeoxyglucose and [^{11}C]deoxyglucose. *J Cereb Blood Flow Metab* 1985;5:179–192.
28. Foster NL, Gilman S, Berent S, et al. Cerebral hypometabolism in progressive supranuclear palsy studied with positron emission tomography. *Ann Neurol* 1988;24:399–406.
29. Gilman S, Junck L, Markel DS, et al. Cerebral glucose hypermetabolism in Friedreich's ataxia detected with positron emission tomography. *Ann Neurol* 1990;28:750–757.
30. Gilman S, Markel DS, Koeppe RA, et al. Cerebellar and brainstem hypometabolism in olivopontocerebellar atrophy detected with positron emission tomography. *Ann Neurol* 1988;23:223–230.
31. Heiss W-D, Pawlik G, Herholz K, et al. Regional kinetic constants and cerebral metabolic rate for glucose in normal human volunteers determined by dynamic positron emission tomography of [^{18}F]-2-fluoro-2-deoxy-D-glucose. *J Cereb Blood Flow Metab* 1984;4:212–223.
32. Halliday GM, Li YW, Blumbergs PC, et al. Neuropathology of immunohistologically identified brainstem neurons in Parkinson's disease. *Ann Neurol* 1990;27:373–385.
33. Otsuka M, Ichiya Y, Hosokawa S, et al. Striatal blood flow, glucose metabolism and [^{18}F]-DOPA uptake: difference in Parkinson's disease and atypical parkinsonism. *J Neurol Neurosurg Psychiatry* 1991;54:898–904.
34. Eberling JL, Richardson BC, Reed BR, et al. Cortical glucose metabolism in Parkinson's disease without dementia. *Neurobiol Aging* 1994;15:329–335.
35. Pickel VM, Beckley SC, John TH, et al. Ultrastructural immunocytochemical localization of tyrosine hydroxylase in the neostriatum. *Brain Res* 1981;225:373–385.
36. Jacobs BW, Butcher LL. Pathology of the basal forebrain in Alzheimer's disease and other dementias. In: Scheibel AB, Wechsler AF, eds. *The biological substrates of Alzheimer's disease.* Orlando: Academic Press; 1986:87–100.
37. Perry RH, Perry EK, Smith CJ, et al. Cortical neuropathological and neurochemical substrates of Alzheimer's and Parkinson's diseases. *J Neural Transm Suppl* 1987;24: 131–136.
38. Huang S-C, Phelps ME, Hoffman EJ, et al. Noninvasive determination of local cerebral metabolic rate of glucose in man. *Am J Physiol* 1980;238:E69–E82.
39. Brownell GL, Kearfott KJ, Kairento AL, et al. Quantitation of regional cerebral glucose metabolism. *J Cereb Blood Flow Metab* 1983;7:919–924.
40. Evans AC, Diksic M, Yamamoto YL, et al. Effect of vascular activity in the determination of rate constants for the uptake of ^{18}F-labeled-2-fluoro-2-deoxy-D-glucose: error analysis and normal values in older subjects. *J Cereb Blood Flow Metab* 1986;6:724–738.
41. Goto I, Taniwaki T, Hosokawa S, et al. PET studies in dementia. *J Neurol Sci* 1993;114:1–6.
42. Kalaria RN, Harik SI. Reduced glucose transporter at the blood-brain barrier and in cerebral cortex in Alzheimer's disease. *J Neurochem* 1989;53:1083–1088.
43. Marcus DL, de Leon MJ, Goldman J, et al. Altered glucose metabolism in microvessels from patients with Alzheimer's disease. *Ann Neurol* 1989;26:91–94.
44. Huang S-C, Phelps ME, Hoffman EJ, Kuhl DE. Error sensitivity of fluorodeoxyglucose method for measurement of cerebral metabolic rate of glucose. *J Cereb Blood Flow Metab* 1981;1:391–401.

PET Measurements of Neuroreceptor Occupancy by Typical and Atypical Neuroleptics

Peter F. Goyer, Marc S. Berridge, Evan D. Morris, William E. Semple, Beth A. Compton-Toth, S. Charles Schulz, Dean F. Wong, Floro Miraldi and Herbert Y. Meltzer

Cleveland Veterans Affairs Medical Center, Cleveland, Ohio; Departments of Radiology and Psychiatry, Case Western Reserve University Medical School and University Hospitals, Cleveland, Ohio; and Department of Radiology, Johns Hopkins University Medical School, Baltimore, Maryland

The goal of this study was to use PET and ^{11}C-N-methylspiperone (^{11}C-NMSP) to measure the differences in relative occupancy of serotonin (5-hydroxytryptamine-2 or 5-HT$_{2A}$) and dopamine-2 (D2) neuroreceptors in subjects being treated with typical or atypical antipsychotic drugs. **Methods:** We used PET and single-dose ^{11}C-NMSP to measure receptor indices and relative receptor occupancy of 5-HT$_{2A}$ receptors in frontal cortex and D2 receptors in basal ganglia in five subjects who were neuroleptic free, five subjects who were being treated with typical antipsychotic drugs and five subjects who were being treated with clozapine, an atypical antipsychotic drug. **Results:** Among the three groups, there were significant differences in 5-HT$_{2A}$ indices, D2 indices and the ratio of 5-HT$_{2A}$ to D2 indices. With no overlap, the 5-HT$_{2A}$ index separated all subjects who received clozapine and the D2 index separated the remaining two groups. **Conclusion:** Typical antipsychotic and atypical antipsychotic subjects do have differing patterns of 5-HT$_{2A}$ and D2 relative receptor occupancy when measured with a single PET scan, single ^{11}C-NMSP radiotracer dose and no separately injected "cold" pharmaceutical.

Key Words: PET; carbon-11-N-methylspiperone; neuroreceptor occupancy

J Nucl Med 1996; 37:1122–1127

Received Mar. 24, 1995; revision accepted Nov. 1, 1995.

For correspondence or reprints contact: Peter F. Goyer, MD, Chief of Staff, Cleveland VAMC (B), 10,000 Brecksville Rd., Brecksville, OH 44141.